ЖЭТФ, 2014, том 145, вып. 5, стр. 830–837

EFFECT OF SURFACE Si–Si DIMERS ON PHOTOLUMINESCENCE OF SILICON NANOCRYSTALS IN THE SILICON DIOXIDE MATRIX

O. B. Gusev [a*], ***A. V. Ershov*** [b], ***D. A. Grachev*** [b], ***B. A. Andreev*** [c], ***A. N. Yablonskiy*** [c]

[a] *Ioffe Physical-Technical Institute, Russian Academy of Sciences*
194021, Saint-Petersburg, Russia

[b] *Lobachevsky State University of Nizhni Novgorod*
603950, Nizhny Novgorod, Russia

[c] *Institute for Physics of Microstructures, Russian Academy of Sciences*
603950, Nizhny Novgorod, Russia

Received November 27, 2013

The effect of surface states of silicon nanocrystals embedded in silicon dioxide on the photoluminescent properties of the nanocrystals is reported. We have investigated the time-resolved and stationary photoluminescence of silicon nanocrystals in the matrix of silicon dioxide in the visible and infrared spectral ranges at 77 and 300 K. The structures containing silicon nanocrystals were prepared by the high-temperature annealing of multilayer SiO_x/SiO_2 films. The understanding of the experimental results on photoluminescence is underlain by a model of autolocalized states arising on surface Si–Si dimers. The emission of autocatalized excitons is found for the first time, and the energy level of the autolocalized states is determined. The effect of these states on the mechanism of the excitation and the photoluminescence properties of nanocrystals is discussed for a wide range of their dimensions. It is reliably shown that the cause of the known blue boundary of photoluminescence of silicon nanocrystals in the silicon dioxide matrix is the capture of free excitons on autolocalized surface states.

DOI: 10.7868/S0044451014050061

1. INTRODUCTION

An intense photoluminescence (PL) of porous silicon in the visible spectral range at room temperature was first observed by Canham in 1990 [1]. This PL, not inherent to silicon (which is an indirect gap semiconductor), was explained as the result of the size quantization effect of electron states in silicon nanocrystals. The possibility to create optoelectronic devices based thereon and the prospects of their use in photovoltaics promoted research on the optical and electric properties of silicon nanocrystals in various matrices [2, 3].

Currently, much attention is attracted to silicon nanocrystals in the matrix of silicon dioxide (SiO_2). This is due to the high thermal and chemical stability of the material and its complete compatibility with the traditional silicon microelectronic technology.

To obtain an efficient emission in the visible and near-IR spectral ranges, the nanocrystals should be of the size not exceeding several nanometers. At this size, the ratio of the nanocrystal surface to its volume is large, and the surface states may significantly affect the excitation and emission mechanisms of the nanocrystals.

It is known that with a decrease in the size of silicon nanocrystals in the SiO_2 matrix, the maximum of the PL band at the room temperature shifts from the IR region only to some "blue boundary" of the wavelength about 0.6 μm (corresponding to the emission energy 2.1 eV), which has not been predicted by theoretical calculations based on the size quantization effect [4]. Yet the PL band of silicon nanocrystals in the silicon nitride matrix (Si_3N_4) undergoes the blueshift up to the ultraviolet region of 0.41 μm (approximately 3 eV) as the size of nanocrystals decreases to 2.6 nm [5]. The blueshift up to 3.5 eV is also observed for the PL of porous silicon when the surface of the crystals is covered with hydrogen [6]. Therefore, the existence of the "blue boundary" of 2.1–2.2 eV for PL of silicon nanocrystals in the silicon dioxide matrix demonstrates a strong effect of the nanocrystal surface on the PL characteristics.

*E-mail: oleg.gusev@mail.ioffe.ru

The most widely spread preparation method of silicon nanocrystals in the matrix of silicon dioxide is the high-temperature annealing of initial films of silicon suboxide SiO_x ($x < 2$), which can be carried out by various procedures [3]. The annealing process induces the separation of the Si and SiO_2 phases with the formation of silicon nanocrystals embedded in SiO_2. The size of silicon nanocrystals depends on the amount of excess Si, as well as on the annealing temperature. The results of the studies of the fine structure of X-ray absorption spectra near the edge structure (XANES) indicate that the nanoparticles obtained by the high-temperature annealing of SiO_x films are silicon nanocrystals surrounded with a thin layer of 0.6–0.8 nm of amorphous SiO_x of variable composition x [7]. This way, several types of structural defects — Si=O, Si–O–Si, Si–O, and surface Si–Si dimers — form on the surface of silicon nanocrystals.

It has been shown in theoretical investigations [8, 9] that the blue boundary of PL for silicon nanocrystals in the SiO_2 matrix can be described with a model of autolocalized exciton states forming on the surface Si–Si dimers. We refer to these states as self-trapped exciton state, STE(Si–Si). We note that according to the calculations, radiative recombination of autolocalized excitons on STE(Si–Si) should result in the appearance of a PL band in the range 1.2–1.5 eV for small silicon nanocrystals in the matrix of silicon dioxide. The observation of this band can become the proof of the suggested model. However, no experimental studies that detected PL of autolocalized excitons on surface Si–Si dimers have appeared until now.

Recently, results were published of an experimental investigation of induced light absorption in silicon nanocrystals, which were explained based on a model of the capture of hot excitons into the autolocalized surface states on the Si–O bond [10]. It was shown that in the time interval about 0.1 ns, a hot exciton from the nanocrystal is captured on the surface metastable state, from which it returns into the nanocrystal. This process was described using a phenomenological model of autolocalized excitons constructed in the framework of a single-mode approximation of Huang–Rhys. The Si–O vibration was taken as the vibration mode where the exciton was localized. We refer to these autolocalized surface excitons as STE(Si–O). Based on this model, the processes of "hot" exciton capture from the nanocrystal into the autolocalized state, the backward return into the nanocrystal by thermoactive tunneling, and the processes of the optical ionization of the exciton and its radiative and nonradiative recombination were theoretically discussed in [10, 11]. The STE(Si–O) model may also explain the blue boundary of the PL in silicon nanocrystals. In [10], no attempts were made to detect PL of the autolocalized exciton. It should also be noted that the study of induced light absorption in a silicon nanocrystal cannot be regarded as a direct method of the investigation of autolocalized states.

The purpose of this paper is to provide experimental evidence for the existence of autolocalized states on the surface of silicon nanocrystals in the matrix of silicon dioxide and to reveal their nature and their influence on PL of free and autolocalized excitons. We investigated the stationary and time-resolved PL of silicon nanocrystals in the matrix of SiO_2 in the visible and IR spectral ranges. The obtained experimental results are well understandable based on the model of autolocalized excitons on surface Si–Si dimers.

2. PREPARATION OF SAMPLES AND MEASUREMENT PROCEDURES

In this work, we studied structures composed of thin films of silicon dioxide containing silicon nanocrystals and separated by layers of pure silicon dioxide. This allowed decreasing a probable effect of energy transfer from a silicon nanocrystal of a smaller size to the nearest-neighbor of a larger size. In thin (close to the size of the silicon nanocrystal) layers of the SiO_2 matrix, the number of nearest neighbors is several times smaller than in the case where the thickness of the SiO_2 layer with silicon nanocrystals is larger than the nanocrystal size.

Multilayer nanostructures a-SiO_x/a-SiO_2 were obtained by alternate evaporation in a vacuum of appropriate initial materials from two separate sources, with the layer thickness monitored photometrically as described in [12, 13]. The a-SiO_x layers were deposited by evaporation of SiO powder from an effusion tantalum source, and the a-SiO_2 layers, by electron beam evaporation of fused silica. The temperature of the silicon substrate during the deposition was maintained at 200 °C. The thickness of a-SiO_2 layers was set at a constant value of 2.8 nm, and the structures were distinguished only by the thickness of a-SiO_x layers. In all cases, the first deposited layer was that of silicon suboxide, followed by SiO_2, a-SiO_x, etc.; the upper layer consisted of SiO_2. After deposition, structures were annealed at high temperature (about 1100 °C) for two hours in an N_2 atmosphere. As a result, structures were obtained with silicon nanocrystals of the mean dimensions 2.5, 3.5, and 4.5 nm, approximately in accordance with the thickness of the deposited layer of

a-SiO_x. The size control of the nanocrystals was carried out with high-resolution transmission electron microscopy as described in [12, 13].

The stationary PL was exited with a semiconductor laser emitting at $\lambda = 405$ nm and was registered by a photomultiplier or by a liquid nitrogen-cooled germanium detector. The time- resolved PL spectra were obtained at the excitation with a pulse nitrogen laser emitting at $\lambda = 337$ nm, with a pulse duration of 7 ns and the repetition frequency 45 Hz. The PL measurements were performed with the use of grating monochromator, a stroboscopic voltmeter with the strobe pulse duration of 4 ns, and a digital oscillograph. The time resolution of the registration system with the use of a photomultiplier tube in the spectral range 400–850 nm was 20 ns, and in the region 700–1600 nm, when the cooled germanium detector was used, 20 μs. All PL spectra are corrected for the spectral sensitivity of the optical system.

3. EXPERIMENTAL RESULTS

In Fig. 1, PL spectra are shown for the three obtained nanoperiodic structures containing ensembles of silicon nanocrystals of mean nanocrystal sizes 2.5, 3.5, and 4.5 nm in the matrix of silicon dioxide. PL was excited with a continuous laser at $\lambda = 405$ nm.

The PL bands with the maxima in the region 700–900 nm are well known for silicon nanocrystals in the SiO_2 matrix. They originate from size quantization of the electron states in silicon nanocrystals. Half-widths of the bands of this PL amount to 250–300 meV and are

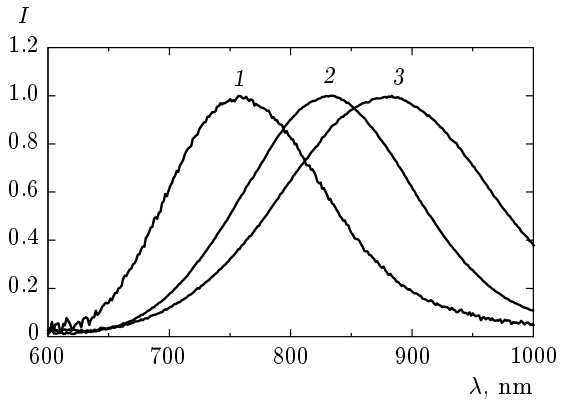

Fig. 1. The normalized PL spectra of silicon nanocrystals in the SiO_2 matrix obtained under excitation with a continuous laser at $\lambda = 405$ nm for the mean size of nanocrystals in the ensemble (*1*) 2.5 nm; (*2*) 3.5 nm, and (*3*) 4.5 nm; $T = 295$ K

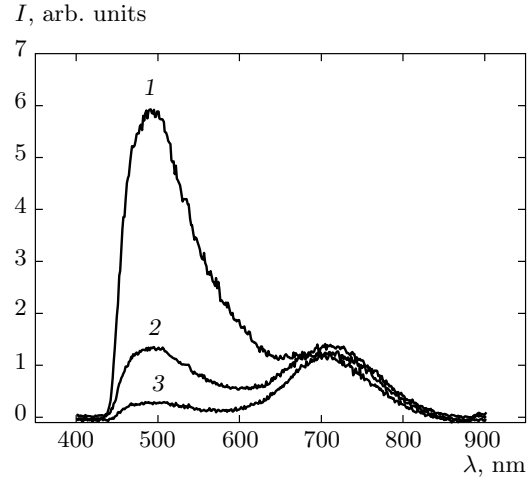

Fig. 2. PL spectra of the structure with silicon nanocrystals of the mean size about 2.5 nm at $T = 295$ K for three delay times with respect to the excitation pulse: (*1*) 0–10 ns, (*2*) 20 ns, (*3*) 40 ns. The left-hand side of the spectrum is cut off by the filter at $\lambda = 450$ nm

practically independent of temperature. We note that in the experiments published in [14], where the PL of one silicon nanocrystal was separated at low temperature, the half-width of the PL band was 20–30 meV. Consequently, the observed width of the PL band (200–300 meV) is mainly due to the dispersion of nanocrystal sizes in the ensemble. This fact allows the study of PL kinetics in a wide range of nanocrystal sizes using silicon-nanocrystal ensembles with one to two different mean sizes, by changing the wavelength of the registered PL signal.

It is well known that under the excitation with a pulse laser, regardless of the nanocrystal size, two PL bands are observed from the silicon nanocrystal in the matrix of SiO_2. In Fig. 2, we present typical PL spectra of our structure with the mean size silicon nanocrystals about 2.5 nm, registered at different delay times with respect to the excitation pulse.

As can be seen from Fig. 2, beside the above-described PL band in the region 700–900 nm, related to size quantization of the electron states in the nanocrystals, a second PL band is observed in the region 500–550 nm. The decay time of this PL band, in keeping with the data of Fig. 2, is of the order of 10 ns (the time resolution limit), three orders of magnitude smaller than the decay time of the PL band in the region 700–900 nm. According to the published data, the decay time of the PL band in the region 500–550 nm amounts to several nanoseconds. The origin of this

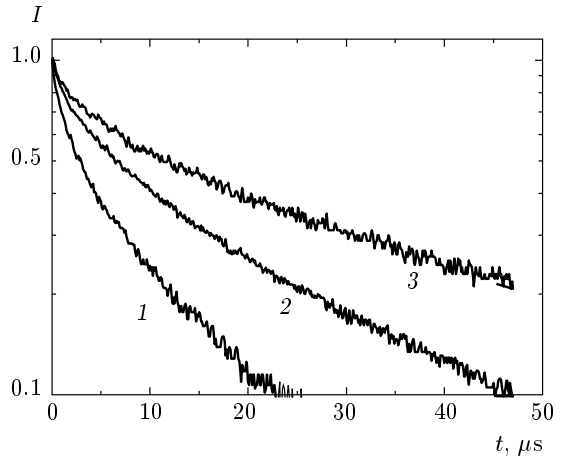

Fig. 3. PL decay curves at three different wavelengths obtained at $T = 295$ K for a sample with the mean size of nanocrystals 2.5 nm: (*1*) 660 nm; (*2*) 720 nm; (*3*) 800 nm

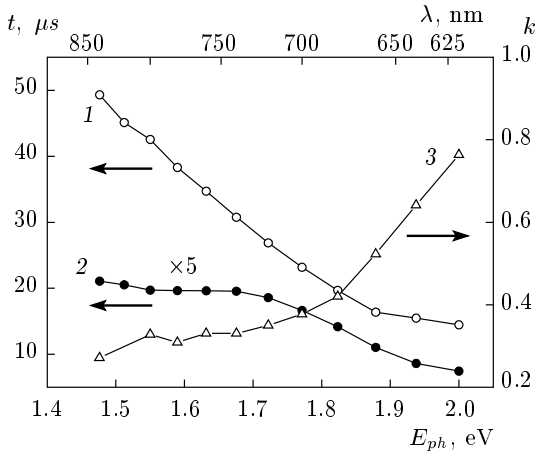

Fig. 4. Decay time of the (*1*) slow and (*2*) fast components of PL for silicon nanocrystals with the mean size 3.5 nm as a function of the energy E_{ph} of emitted photon. Plot (*3*) shows the fraction k of the amplitude of the fast component in the overall PL amplitude ($k = A_{fast}/(A_{fast} + A_{slow})$). The results were obtained at $T = 300$ K. The points are connected with lines for clarity

band was not established. It is usually attributed to the Si=O bonds on the interface between the silicon nanocrystal and the SiO_2 matrix. We note that as can be seen from Fig. 2, we did not observe a time delay (within an accuracy of 20 ns) in the appearance of PL in the region 700–900 nm originating from the size quantization effect of the electron states in nanocrystals.

The principal attention in this research was focused on the study of the decay kinetics of free excitons PL in the region 850–650 nm (1.45–1.9 eV), presuming that the selection of PL according to wavelength in this range would correspond to the kinetic dependences of the emission for the nanocrystals of respective sizes. The example of the PL kinetics for silicon nanocrystals at several energies of emitted photons for a sample with the mean size of nanocrystals 2.5 nm is shown in Fig. 3.

It follows from Fig. 3 that the PL decay of silicon nanocrystals is not of the single-exponential character. The impossibility to describe the PL decay observed for silicon nanocrystals in the silicon dioxide matrix with a single exponent is commonly overcome by applying a "stretched" exponent. This character of decay was attributed to the effect of surface states or to the excitation energy transfer to the nearest neighboring nanocrystal. However, it was shown in [15] that even at the low density of nanocrystals, when energy transfer between nanocrystals could not occur, the PL decay also did not fit the single-exponential behavior. Therefore, the cause of the deviation of the PL decay of silicon nanocrystals in the matrix of SiO_2 from the single-exponential character should be sought in the effect of the surface.

The processing of our experimental data on the PL decay of silicon nanocrystals in the region 850–650 nm (1.45–1.9 eV) has demonstrated that they are well described in the full studied range of photon energies with two exponentials differing in time by approximately an order of magnitude. In Fig. 4, the decay times of the fast and slow PL components of free excitons for the structure with the mean size of nanocrystals 3.5 nm are presented as functions of the energy of the emitted photon (i. e., of the silicon nanocrystal size). In the same figure, the fraction k of the amplitude of the fast component in the total amplitude is also shown.

4. DISCUSSION

The results of our research can be understood based on the model of autolocalized exciton states on surface Si–Si dimers STE(Si–Si), developed in [8, 9]. Surface Si–Si dimers arise at the replacement of a silicon atom with an oxygen atom, with the formation of chemical bonds with two neighboring silicon atoms giving a bridging Si–O–Si bond. Two remaining dangling bonds of the silicon form bonding and antibonding orbitals of the dimer. We note that in theoretical calculations of the energy of formation of Si–O, Si–O–Si, and Si=O bonds on the surface of nanocrystals, the bridging bond was shown to lead to the most stable isomeric configuration. In the case of the bridging structure, deforma-

tion is localized around the Si–O–Si bond, thus producing the stretching of the Si–Si dimer [16, 17]. The Si–Si dimers on the surface of the oxidized silicon were recently found by detecting the electron spin resonance spectra using the effect of spin-dependent recombination [18].

In the framework of this model, we believe that the results of the fitting the PL decay curves with two exponentials presented in Fig. 4 (curves *1* and *2*) allow suggesting that the nanocrystal ensemble contains two groups of emitting nanocrystals. The first group consists of the nanocrystals that have surface states (states of autolocalized excitons) where free excitons can be captured, and the second group consists of the nanocrystals of the same size devoid of these surface states. Just the presence of these two groups of nanocrystals results in the two-exponential PL decay of silicon nanocrystals. The slow component of the PL decay (curve *1* in Fig. 4) is due to the well-known increase in the rate of radiative recombination at decreasing the nanocrystal size. The experimental data on the slow component (curve *1* in Fig. 4) are well consistent with the known lifetime of PL of silicon nanocrystals of the corresponding size. As regards the fast component of the PL decay (curve *2* in Fig. 4), whose amplitude increases with decreasing the size of nanocrystals (curve *3* in Fig. 4), we attribute it to the reduced lifetime of free excitons in the nanocrystals having the surface STE states.

We qualitatively discuss the effect of the size of nanocrystals with surface Si–Si dimers on possible transitions between the free and autolocalized excitons and their radiative recombination. In Fig. 5, the configuration coordinate diagram is presented for three characteristic sizes of nanocrystals having surface Si–Si dimers. The shape of the adiabatic potentials for Si–Si dimers shown in Fig. 5 corresponds to the theoretical calculations in [8, 9] with the strong anharmonicity due to the stretching of the covalent Si–Si bond on the silicon nanocrystal surface taken into account.

Under optical excitation, the "hot" excitons arise in all nanocrystals of the ensemble regardless of the presence or absence of surface Si–Si dimers in them. After the thermalization process, we arrive at the adiabatic potentials FE1, FE2, and FE3 shown in Fig. 5, which correspond to the presence of a free exciton in the nanocrystals with surface Si–Si dimers. We note that the capture of "hot" excitons into the autolocalized state STE(Si–Si) is excluded because the excited oscillation levels of the Si–Si dimer exist only in a narrow interval of energies (cf. Fig. 5).

The process of excitation of free excitons in nanocrystals with STE(Si–Si) states is therefore essentially different from the excitation process of free excitons in nanocrystals with STE(Si–O) states; for the latter, the capture of "hot" excitons into the autolocalized state with the subsequent transition into free-exciton states plays the decisive role [8, 9].

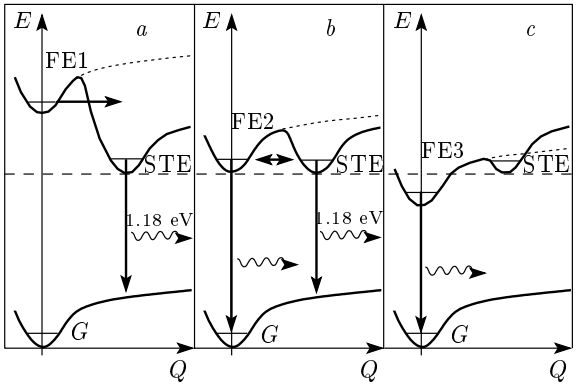

Fig. 5. Schematic configuration coordinate diagram for three characteristic sizes of nanocrystals having STE(Si–Si) states. The configuration coordinate Q corresponds to the stretching of the covalent Si–Si bond on the silicon nanocrystal surface. The adiabatic potential G corresponds to a Si–Si dimer with no exciton. The adiabatic potentials FE1 > FE2 > FE3 are presented in the cases where a free exciton is present in the nanocrystal of the respective size $D1 < D2 < D3$. The adiabatic potential of STE(Si–Si) corresponds to the presence of an exciton in the autolocalized surface state. The vertical arrows show the possible radiative recombination transitions and the horizontal arrows show the possible nonradiative transitions of free excitons into the autolocalized state, and the reverse transition

We first consider the case of the smallest nanocrystals, where the energy minimum of the adiabatic potential (FE1) for a free exciton is higher than the energy of the STE(Si–Si) state (cf. Fig. 5*a*). Free excitons due to the low potential barrier separating the minima of the adiabatic potentials FE1 and STE easily go over to the autolocalized state. Photoluminescence of free excitons from these nanocrystals would be weak or even absent. This phenomenon very well explains the fact of the blue boundary of PL of silicon nanocrystals in the silicon dioxide matrix at the dimensions of nanocrystals smaller than 2 nm (emission energy near 2 eV) [8].

The total lifetime τ of free excitons in small nanocrystals with STE(Si–Si) states is governed by the radiative lifetime τ_r and by the time τ_{ta} of the thermally activated transition in the autolocalized state:

$$\frac{1}{\tau} = \frac{1}{\tau_r} + \frac{1}{\tau_{ta}}. \qquad (1)$$

For $\tau_r \gg \tau_{ta}$ (low barrier), we have $\tau = \tau_{ta}$. Therefore, the fast component of the PL decay time of free excitons shown in Fig. 4 is determined by the time of capture of free excitons into the STE state. As the nanocrystal size increases, τ_{ta} increases due to the increase in the potential barrier between the state of the free exciton and STE state. This is fully consistent with the results of measuring the decay time of the fast PL component in the range 1.7–1.9 eV (cf. Fig. 4).

At the largest sizes of the nanocrystals from the ensemble (cf. Fig. 5*c*), when the energy of the free exciton FE3 is lower than the energy of the autolocalized state, the energy barrier separating free-exciton states and STE states is large. In this case, the free excitons cannot be captured into the STE states. This means that the probability of the radiative recombination of free excitons in these nanocrystals is insensitive to the presence of the surface Si–Si dimers.

When the energy of the free exciton from the nanocrystal in the ensemble coincides with the energy of an STE state (cf. Fig. 5*b*), the energy barrier separating the state of the free exciton and the STE state is identical for the free and autolocalized excitons. The free excitons can transit into the STE states, and the autolocalized excitons, into free-exciton states. We believe that the energy range where the decay time of the fast PL component (cf. Fig. 4, curve *2*) is independent of the energy corresponds just to this case. It is therefore possible to estimate the energy position of the autolocalized state to be close to 1.7 eV (730 nm). Approximately the same value was obtained from the dependence of the amplitude ratio of the fast and slow components on the energy of the emitted photon (cf. Fig. 4, curve *3*). We note that the energy of 1.7 eV corresponds to the emission energy of silicon nanocrystals in SiO_2, below which the quantum efficiency of silicon nanocrystals starts to increase from 0.5 at 700 nm (1.8 eV) to approximately 1 at 800 nm (1.5 eV) [19].

5. EMISSION OF AUTOLOCALIZED EXCITONS ON A SURFACE Si–Si DIMER

We believe the applied model of STE(Si–Si) states can be proved by experimentally detecting the PL band of an autolocalized exciton whose intensity is maximum for small nanocrystals where the energy minimum of the adiabatic potential FE1 for a free exciton is located higher than the energy of the STE(Si–Si) state (cf. Fig. 5*a*).

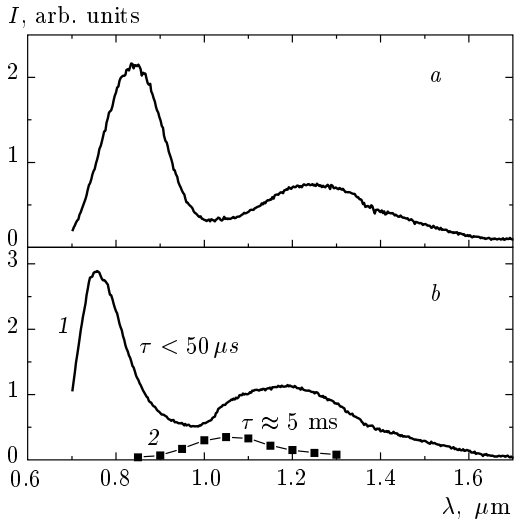

Fig. 6. PL spectra of the structure with the mean size of silicon nanocrystals (*a*) 3.5 nm and (*b*) 2.5 nm: (*1*) the complete PL spectrum; (*2*) the PL band extracted from spectrum *1* corresponding to the large decay time $\tau \approx 5$ ms; $T = 77$ K

We have found the PL of an autolocalized exciton when investigating the PL of two structures with the mean size of nanocrystals 2.5 and 3.5 nm. Photoluminescence was excited with the radiation of a GaN laser emitting at $\lambda = 405$ nm. The laser was modulated with a current to obtain a pulse duration of 50 ms at the frequency 10 Hz. In this case, PL was registered with a cooled germanium photodetector. The PL spectra of the structures with the mean size of nanocrystals 2.5 and 3.5 nm registered at the temperature 77 K are presented in Fig. 6.

As can be seen from Fig. 6, along with the PL band of the free excitons with the maxima at 0.825 and 0.735 μm, bands with the maxima at 1.24 and 1.18 μm for nanocrystals of the respective size 3.5 and 2.5 nm are observed in the spectra of both structures. The same as the peak of free excitons, the low-energy peak is subject to the blueshift with decreasing the size of nanocrystals. The shift of the low-energy peak amounts to about a half of the blueshift of the free-exciton PL band. The longwave bands were attributed in [20] to the recombination of an electron from the valence band with a hole located in a deep surface trap on the boundary between the silicon nanocrystal and SiO_2. In this model, the half-shift corresponds to the shift of the edge of the conduction band of silicon nanocrystals.

We see from Fig. 6 that the PL spectra of the structures have a nontrivial shape of the PL bands in the region 0.9–1.1 μm, especially evident for the structure

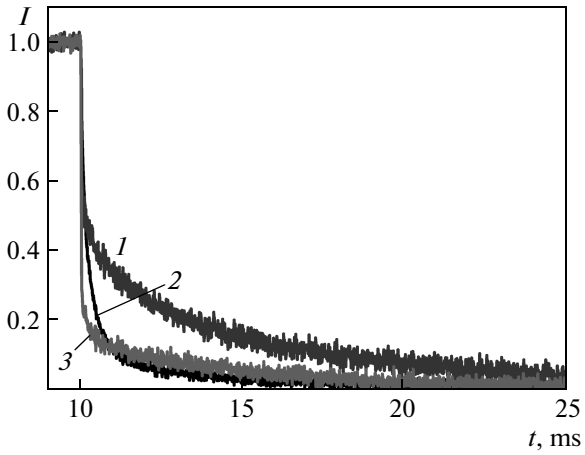

Fig. 7. PL decay curves at the wavelengths (*1*) 1.05 μm, (*2*) 0.85 μm, and (*3*) 1.20 μm for a sample with the mean size of nanocrystals 2.5 nm; $T = 295$ K

with the mean size of nanocrystals 2.5 nm (cf. Fig. 6*b*). The spectrum shape suggests the existence of one more band in this region. To discover this band, we have studied the PL kinetics depending on the energy of the emitted photon in the region 0.8–1.25 μm. Examples of PL decay curves in the region 0.9–1.2 μm for a sample with the mean size of nanocrystals 2.5 nm are shown in Fig. 7.

As can be seen from Fig. 6, the PL decay is governed by two components: a short one with the time less than 50 μs, and a long one with the time about 5 ms in the whole spectral range where this band is observed. This large difference in the decay times permits an easy extraction of the long-lived PL component, whose spectrum is shown in Fig. 6*b* (curve *2*). We believe that the PL band discovered in the region 0.9–1.2 μm with the maximum at about 1.05 μm (1.18 eV) and the FWHM about 250 meV is caused by radiative recombination of the autolocalized excitons. The energy position of this band is in good agreement with the position theoretically calculated for an exciton localized on a surface Si–Si dimer [8, 9].

We interpreted the long lifetime of the autolocalized excitons at 77 K and the absence of the corresponding emission band at room temperature based on the model of Calcott et al. [21]. This model takes into account that the exciton levels are split by the energy of the exchange interaction between an electron and a hole into a triplet (lower) and a singlet (upper) level. The radiative transition from the triplet level is forbidden. It is known that the level splitting energy of free excitons in silicon nanocrystals in SiO_2 monotonically increases from 8.4 to 17 meV as the nanocrystals size decreases from 5.5 to 2 nm [20, 22]. As a result, at helium temperatures, where the free exciton exists in the triplet state, its radiative lifetime is large, 5–10 ms.

It can be expected that the energy of the exchange splitting of the autolocalized state of a surface exciton should be larger. From the obtained decay time $\tau = 2$ ms of the long-lived PL band of the autolocalized exciton, we can estimate the energy of the singlet–triplet splitting of STE(Si–Si). For this, we use the formula describing the temperature dependence of the PL radiative lifetime τ from [6],

$$\frac{1}{\tau} = \left[\frac{3}{\tau_t} + \frac{1}{\tau_s}\exp\left(-\frac{\Delta E}{k_B T}\right)\right] \times \left[3 + \exp\left(-\frac{\Delta E}{k_B T}\right)\right]^{-1}, \quad (2)$$

where τ_s and τ_t are the radiative lifetimes of the exciton in the singlet and triplet states, k_B is the Boltzmann constant, and ΔE is the energy splitting. For the estimation, we took $\tau_s = 10$ ns, the characteristic lifetime of direct radiative transitions not involving phonons, and $\tau_t = 5$ ms, the characteristic lifetime of a free exciton in the triplet state, and the lifetime of the autolocalized exciton, which we experimentally measured as $\tau = 5$ ms at temperature 77 K. The obtained estimation of the energy of the singlet–triplet splitting, $\Delta E = 60$–80 meV, was, as expected, larger than in the case of a free exciton in silicon nanocrystals, where its value ranged from 6 to 20 meV for nanocrystals of the size from 5 to 2 nm. This is due to the stronger exchange interaction originating from the exciton localization on the nanocrystal surface within the area less than 1 nm.

6. CONCLUSION

We have studied the kinetics of PL decay of silicon nanocrystals in the matrix of silicon dioxide in a wide range of the energy of emitted photons (nanocrystals sizes). The experimental results are well consistent with the model of the capture of free excitons on surface Si–Si dimers with the formation of autolocalized excitons, calculated theoretically in [8, 9]. The PL band of the autolocalized exciton in the SiO_2 matrix with silicon nanocrystals is discovered for the first time. The energy position of the autolocalized exciton (1.7 eV), the energy of splitting of singlet–triplet states (60–80 meV), and the energy of the optical transition of the autolocalized exciton (1.18 eV) are estimated. It is

shown that the surface Si–Si dimers essentially govern the luminescence properties of silicon nanocrystals in the SiO_2 matrix, determining the "blue boundary" of PL of silicon nanocrystals and the high quantum yield of the nanocrystals with the emission energy below the energy level of the autolocalized exciton state.

The authors thank I. N. Yassievich and L. S. Vlasenko for the fruitful discussions. The authors express their gratitude to I. A. Karabanova and I. A. Chugrov for the technical help in the preparation of the studied structures. The study was partially supported by the RFBR (grant № 14-02-00119-a) and by the Program of the Department of Physical Sciences "Physics of New Materials and Structures".

REFERENCES

1. L. T. Canham, Appl. Phys. Lett. **57**, 1046 (1990).

2. A. A. Ishchenko, G. V. Fetisov, and L. A. Aslanov, *Nanosilicon*: *Properties, Preparation, and Application; Investigation and Control Methods*, Fizmatlit, Moscow (2011) [in Russian].

3. L. Khriachtchev, *Silicon Nanophotonics, Basic Principles, Present Status, and Perspectives*, World Sci., Singapore (2009).

4. P. M. Fauchet, Materials Today **8**, 26 (2005).

5. T-Y. Kim, N.-M. Park, K.-H. Kim et al., Appl. Phys. Lett. **85**, 5355 (2004).

6. D. Kovalev, H. Heckler, G. Polisski et al., Phys. Stat. Sol. (b) **215**, 871 (1999).

7. N. Daldosso, M. Luppi, S. Ossicini et al., Phys. Rev. B **68**, 085327 (2003).

8. C. Delerue and M. Lanoo, *Nanostructures*: *Theory and Modelling*, Springer-Verlag, Berlin (2004).

9. G. Allan, C. Delerue, and M. Lannoo, Phys. Rev. Lett. **76**, 2961 (1996).

10. W. D. A. M. de Boer, D. Timmerman, T. Gregorkiewicz et al., Phys. Rev. B **85**, 161409(R) (2012).

11. A. V. Gert and I. N. Yassievich, Pis'ma v Zh. Eksp. Teor. Fiz. **97**, 93 (2013).

12. A. V. Ershov, D. I. Tetel'baum, I. A. Chugrov et al., Fiz. i Tekhn. Poluprovodnikov **45**, 747 (2011).

13. A. V. Ershov, I. A. Chugrov, D. I. Tetel'baum et al., Fiz. i Tekhn. Poluprovodnikov **47**, 460 (2013).

14. I. Sychugov, R. Juhasz, J. Valenta et al., Phys. Rev. Lett. **94**, 087405 (2005).

15. O. Guillois, N. Herlin-Boime, C. Reynaud et al., J. Appl. Phys. **95**, 3677 (2004).

16. M. Gatti and G. Onida, Phys. Rev. B **72**, 045442 (2005).

17. *Silicon Nanocrystals*: *Fundamentals, Synthesis, and Applications*, ed. by L. Pavesi and R. Turan, Wiley–VCH Verlag, Weinheim (2010), p. 5.

18. M. Otsuka, T. Matsuoka, L. S. Vlasenko et al., Appl. Phys. Lett. **103**, 111601 (2013).

19. S. Miura, T. Nakamura, M. Fujii et al., Phys. Rev. B **73**, 245333 (2006).

20. S. Takeoka, M. Fujii, and S. Hayashi, Phys. Rev. B **62**, 16820 (2000).

21. P. D. J. Calcott, K. J. Nash, L. T. Canham et al., J. Phys.: Condens. Matter **5**, L91 (1993).

22. M. L. Brongersma, P. G. Kik, A. Polman et al., Appl. Phys. Lett. **78**, 351 (2000).